

Impact of target warhead and linkage vector on inducing protein degradation: comparison of Bromodomain and Extra-Terminal (BET) degraders derived from triazolodiazepine (JQ1) and tetrahydroquinoline (I-BET726) BET inhibitor scaffolds

Kwok-Ho Chan, Michael Zengerle, Andrea Testa, and Alessio Ciulli

J. Med. Chem., **Just Accepted Manuscript** • Publication Date (Web): 08 Jun 2017

Downloaded from <http://pubs.acs.org> on June 8, 2017

Just Accepted

“Just Accepted” manuscripts have been peer-reviewed and accepted for publication. They are posted online prior to technical editing, formatting for publication and author proofing. The American Chemical Society provides “Just Accepted” as a free service to the research community to expedite the dissemination of scientific material as soon as possible after acceptance. “Just Accepted” manuscripts appear in full in PDF format accompanied by an HTML abstract. “Just Accepted” manuscripts have been fully peer reviewed, but should not be considered the official version of record. They are accessible to all readers and citable by the Digital Object Identifier (DOI®). “Just Accepted” is an optional service offered to authors. Therefore, the “Just Accepted” Web site may not include all articles that will be published in the journal. After a manuscript is technically edited and formatted, it will be removed from the “Just Accepted” Web site and published as an ASAP article. Note that technical editing may introduce minor changes to the manuscript text and/or graphics which could affect content, and all legal disclaimers and ethical guidelines that apply to the journal pertain. ACS cannot be held responsible for errors or consequences arising from the use of information contained in these “Just Accepted” manuscripts.

1
2
3
4
5
6
7
8
9
10
11
12
13
14
15
16
17
18
19
20
21
22

Impact of target warhead and linkage vector on inducing protein degradation: comparison of Bromodomain and Extra-Terminal (BET) degraders derived from triazolodiazepine (JQ1) and tetrahydroquinoline (I-BET726) BET inhibitor scaffolds

23 Kwok-Ho Chan, Michael Zengerle, Andrea Testa, Alessio Ciulli*

24
25
26
27
28
29 Division of Biological Chemistry and Drug Discovery, School of Life Sciences, University of
30 Dundee, Dow Street, Dundee, DD1 5EH, Scotland, UK.
31
32

33
34
35
36
37 * Correspondence and requests for materials should be addressed to A.C. E-mail:

38 a.ciulli@dundee.ac.uk
39
40
41
42
43
44
45
46
47

48 **KEYWORDS:** protein degradation, PROTACs, bromodomain, cooperativity, acute myeloid
49 leukemia
50
51
52
53
54
55
56
57
58
59
60

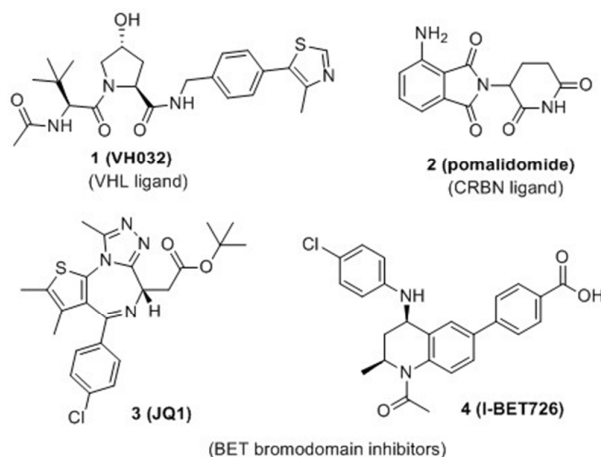
ABSTRACT

The design of proteolysis-targeting chimeras (PROTACs) is a powerful small-molecule approach for inducing protein degradation. PROTACs conjugate a target warhead to an E3 ubiquitin ligase ligand via a linker. Here we examined the impact of derivatizing two different BET bromodomain inhibitors, triazolodiazepine JQ1 and the more potent tetrahydroquinoline I-BET726, via distinct exit vectors, using different polyethylene glycol linkers to VHL ligand VH032. Triazolodiazepine PROTACs exhibited positive cooperativities of ternary complex formation, and were more potent degraders than tetrahydroquinoline compounds, which showed negative cooperativities instead. Marked dependency on linker length was observed for BET-degrading and cMyc-driven antiproliferative activities in acute myeloid leukemia cell lines. This work exemplifies as a cautionary tale how a more potent inhibitor does not necessarily generate more potent PROTACs, and underscores the key roles played by the conjugation. The provided insights and framework for structure-activity relationships of bivalent degraders is anticipated to have wide future applicability.

INTRODUCTION

Targeted protein degradation by exploiting the ubiquitin proteasome system has recently emerged as a new modality of intervention for medicinal chemistry.¹⁻³ One approach to induce protein degradation is to design hetero-bifunctional molecules called proteolysis-targeting chimeras (also known as PROTACs) which comprise of a ligand binding an E3 ubiquitin ligase conjugated to a ligand binding the target protein.^{4,5} First introduced by Crews and Deshaies in 2001 (ref. ⁶), developments of the technology over the following decade were in large part hampered by poor drug-likeness of the early generation compounds that typically incorporated peptidic binders for E3 ligases.^{6,7} Recently discovered high-affinity small molecules for the Cullin RING E3 ubiquitin ligases (CRLs),⁸ in particular against von Hippel-Lindau (VHL e.g. **1** (VH032), **Chart 1**)⁹⁻¹¹ and cereblon (CRBN e.g. **2** (pomalidomide), **Chart 1**)¹²⁻¹⁵ greatly contributed to full realization of the technology's potential. As a result of these developments, we and others recently reported potent activities and specificity in cells and *in vivo* of both VHL-based^{5,16-20} and CRBN-based^{18,20-25} PROTACs against several targets – including the Bromodomain and Extra-Terminal (BET) proteins Brd2, Brd3 and Brd4.^{16,19,21,22} BET proteins are particularly attractive targets, with a dozen of BET inhibitors from different scaffolds,^{26,27} that are in >20 clinical trials against a variety of diseases, mainly solid and hematological cancers including acute myeloid leukaemia (AML) and mixed lineage leukemia (MLL)^{28,29} as well as NUT-midline carcinomas.³⁰ BET-targeting PROTACs could provide advantageous therapeutic profiles over BET inhibitors.¹⁹ In addition to their therapeutic potential, BET-targeting PROTACs provide useful chemical tools for posttranslational protein knockdown. The acute, profound and reversible effect of compounds make it an alternative and advantageous approach to genetic knockdowns to study the function of BET proteins in physiological and disease cellular state.

Chart 1. Chemical structures of ligands for VHL (1)¹⁰ and CRBN (2) and BET inhibitors 3 (JQ1)³⁴ and 4 (I-BET726)³⁶.



One potential advantage of transforming inhibitors into degraders using the PROTAC approach is that removal of the entire protein is expected to be mechanistically different from blockade of a single domain interaction with an inhibitor, and to more closely phenocopy genetic downregulation. This limitation is exemplified by small-molecule inhibitors of the bromodomain of SMARCA2 and SMARCA4, which fail to display the antiproliferative phenotype expected based on genetic protein knockdown.³¹ A second advantage of ligand directed protein degradation is the potential to enhance selectivity of target modulation over and above the binary target engagement selectivity of the constitutive inhibitor.^{5,16} Selective targeting of a single BET protein while sparing its paralogs would allow to better decipher their individual physiological roles.³² This is particularly relevant given traditional genetic techniques have proven challenging, exemplified by the embryonic lethality of BET gene knock-outs.³⁰ While selective inhibition of BET bromodomains can be achieved using allele-selective bump-and-hole approaches,³³ single-point mutations need to be introduced ideally using isogenic knock-ins to enable selective target inhibition.

We previously reported VHL-targeting PROTAC compounds **6** (MZ1) and analogue **7** (MZ2) (**Chart 2**, see ref. ¹⁶) that induced preferential depletion of a single BET member, Brd4, over Brd2 and Brd3, despite binding the different BET bromodomains with comparable affinities.¹⁶ Our recent work disclosing the crystal structure of VHL-**6**-Brd4

1
2
3 ternary complex, the first crystal structure of a PROTAC bound to both target protein and E3
4
5 ligase, showed how PROTAC **6** folds into itself to allow the two proteins to form productive
6
7 interactions.⁵ Our discovery provided structural insights into ligand-induced protein-protein
8
9 interactions driving cooperative and preferential formation of ternary complexes as a basis
10
11 for effective target degradation.⁵ This realization has important implications for PROTACs,
12
13 as it demonstrates an added layer of target depletion selectivity through PROTAC-induced
14
15 interactions between the target and the ligase, and supports important roles for the
16
17 derivatization mode of the two warhead ligands via the linker. All BET-degrading PROTACs
18
19 reported so far by us and others^{16,19,21,22} are based on the pan-selective triazolodiazepine-
20
21 based BET inhibitor **3** (**Chart 1**).³⁴ However, while this manuscript was under review, a
22
23 study has reported active CRBN-based BET degraders based on an azacarbazole containing
24
25 BET inhibitor.³⁵ To interrogate the impact of using a different, more potent BET inhibitor
26
27 than **3**, and of exploring a different vector out of the warhead, on the activity and intra-BET
28
29 selectivity profile of BET-targeting PROTACs, we here report novel VHL-recruiting
30
31 PROTACs derived from a high-affinity BET ligand, the tetrahydroquinoline-based BET
32
33 inhibitor **4** (**Chart 1**).³⁶
34
35
36
37
38
39
40
41
42
43
44
45
46
47
48
49
50
51
52
53
54
55
56
57
58
59
60

RESULTS AND DISCUSSION

Crystal structures of **4** (K_d for Brd4 tandem bromodomain = 4 nM;³⁶ compare to K_d s 100 nM for **3**, ref. ³⁴) bound to BET bromodomains show that the free carboxylic acid of the BET inhibitor is solvent exposed and is not involved in direct interactions with the protein (**Figure 1b**).^{36,37} We therefore hypothesized that the carboxylate group could be exploited to readily conjugate a linker e.g. via amide bond formation, without impairing binding to BET bromodomains. Superposition of the co-crystal structures of **3** and **4** each bound to the N-terminal bromodomain of Brd4 (**Figure 1**) additionally showed that the benzoic acid group of **4** extends in a different direction from the *tert*-butyl ester group of **3**. We therefore became interested in exploring the tolerance of the PROTAC approach to different exit vectors from BET inhibitor scaffolds. Based on this design strategy, **4** was connected to the terminal acetamide group of VHL ligand **1** (ref. ¹⁰) to obtain PROTACs **8** (MZP-61), **9** (MZP-54), and **10** (MZP-55) which bear a 2-, 3- and 4-unit PEG linker, respectively, consistently with **5** (MZ4), **6** and **7** (**Chart 2**). Cereblon-based compound **11** (**Chart 2** ref. ²²) was also included to provide a first direct comparison with VHL-based PROTACs.

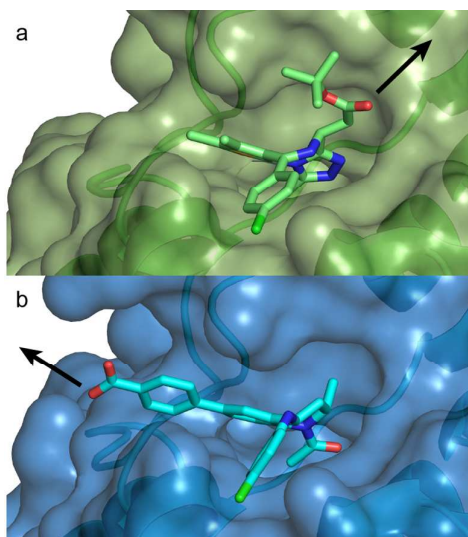
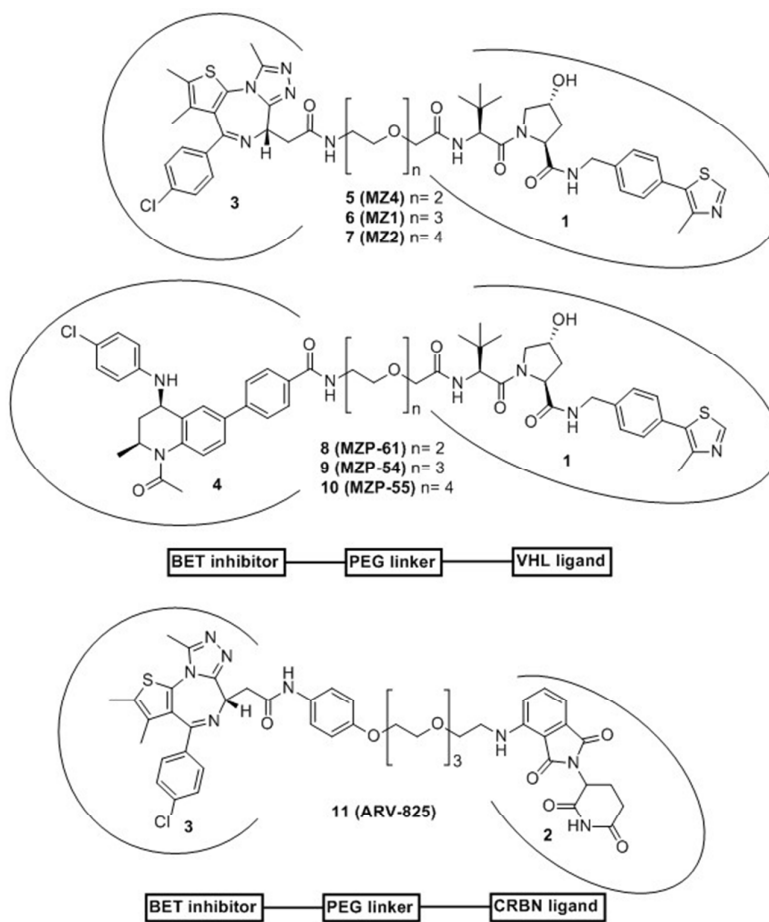


Figure 1. Co-crystal structures to guide PROTAC linking design. First bromodomain of Brd4 with bound (a) **3** (green carbons, PDB code 3MXF³⁴) and (b) **4** (cyan carbons, 4BJX³⁷). Arrows highlight exit vectors for linking.

Chart 2. Chemical structures of VHL-targeting PROTACs based on **4** and **3** used in this study and chemical structure of CRBN-targeting PROTAC **11** (ARV-825).



To assess BET degradation activities, compounds were first profiled in HeLa cancer cells because these cells are less susceptible to the cytotoxic effects of BET knockdown or inhibition (**Figure 2** and **Fig. S1**, see full blots in **Fig. S5**). Representative PROTACs **10** and **7** (each containing a PEG-4 linker unit) induced marked concentration-dependent knockdown of BET proteins (**Figure 2**).

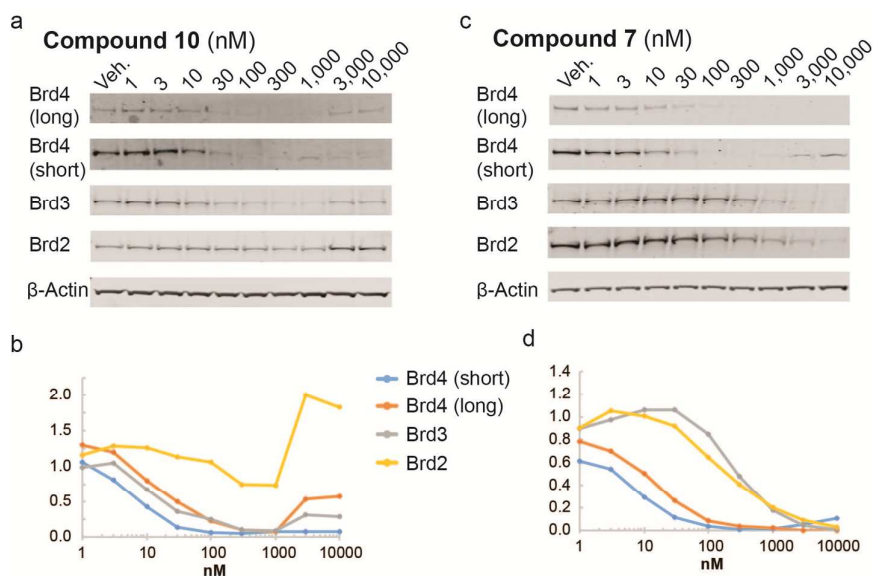


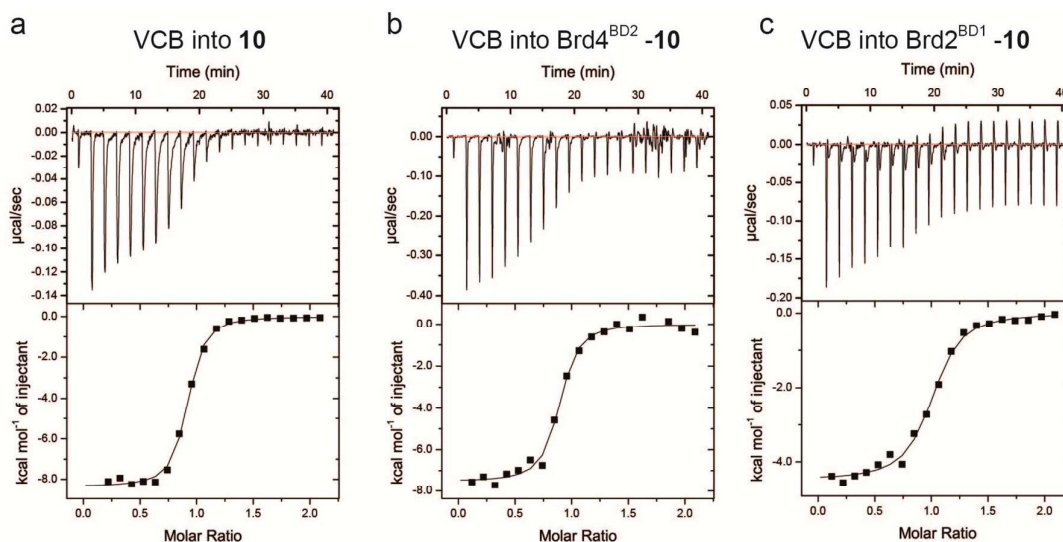
Figure 2. Protein degradation profile of VHL-based BET degraders. HeLa cells were treated for 24 h. Protein levels are shown from one representative of two biological replicates, visualized by immunoblot (a,c) and quantified relative to DMSO control (b,d). Intensity values were quantified as described in the Methods.

Interestingly, tetrahydroquinoline-based compound **10** showed depletion selectivity for Brd4 and Brd3 over Brd2, in contrast to **7** that is a Brd4-selective degrader (**Figure 2**).¹⁶ A similar pattern of BET proteins degradation was observed with PEG-3 linked compounds **9** and **6** (**Fig. S1c-d,g-h**). In contrast, PEG-2 linked PROTACs **5** (**Fig. S1e-f**), and **8** (**Fig. S1a-b**) showed lower activity over all BET proteins. Similar to tetrahydroquinoline-based PROTACs, **11** showed some preference for degrading Brd3/4 over Brd2, although all BET proteins were potently depleted at 100 nM (**Fig. S1i-j**). Interestingly, treatments with tetrahydroquinoline-based PROTACs **9** and **10**, revealed increased levels of BET proteins at the higher concentration (1-10 μ M, **Fig. S1c-d** and **Figure 2a-b**), thought to be due to the “hook effect”.⁴ Brd2 levels even increased beyond vehicle control level (**Fig. S1c-d** and **Figure 2a-b**). These effects were largely recapitulated when the degradation assays were repeated with shorter treatments of 6 h (**Fig. S2**), suggesting that the observed increase in protein levels are not due to secondary effects at the longer time point. Control treatments with the parent BET inhibitors **3** and **4** also led to increased levels of BET proteins (**Fig. S1k-**

1
2
3 n). Marked up-regulation was seen for Brd2 with inhibitor **4** treatment (**Fig. S1k-l**) and for
4
5 Brd4 long isoform with inhibitor **3** (**Fig. S1m-n**). Similar up-regulation of Brd4 with **3** were
6
7 observed in Burkitt's lymphoma cell lines.²² Together, the data suggest that
8
9 tetrahydroquinoline based PROTACs function more as inhibitors than as degraders at the
10
11 higher concentrations. These results underscore the importance to identify suitable
12
13 concentrations to dissect effects due to PROTAC-induced degradation activity from those
14
15 due to inhibitory activity and potential cellular feedback mechanisms, which could
16
17 compensate pharmacological activity. Nonetheless, compounds **9** and **10** act as selective
18
19 degraders of BRD3/4 within appropriate window of concentration (30-100 nM).
20
21

22
23 The distinctive activity profile of tetrahydroquinoline-based PROTACs prompted us
24
25 to compare and contrast thermodynamics of ternary complex formation equilibria for this
26
27 class of PROTACs relative to the triazolodiazepine-based series. We applied an isothermal
28
29 titration calorimetry (ITC) based assay set-up that we recently developed to circumvent
30
31 potential hook-effects in ternary complex formation, and that we used to characterize
32
33 thermodynamics and cooperativities for binding of **6** to VHL and different BET
34
35 bromodomains.⁵ In our previous work, we showed how **6** forms highly cooperative and stable
36
37 complexes between VHL and BET bromodomains, and preferentially with the second
38
39 bromodomain of Brd4 (Brd4^{BD2}).⁵ We therefore set out to measure dissociation constants K_{dS}
40
41 of binary and ternary complexes formed between compounds **5–10**, the VHL-EloC-EloB
42
43 protein (VCB), and Brd4^{BD2}, and the resulting cooperativities (**Table 1**, see also **Fig. S3**). At
44
45 the binary level, the bromodomain warhead of the PROTACs **8–10** bound the BET
46
47 bromodomain consistently with higher potency than the corresponding bromodomain ligand
48
49 warhead within **5–7**, while the VHL ligand warhead bound VCB with comparable affinities
50
51 across all PROTACs (**Table 1**). However strikingly, all tetrahydroquinoline based PROTACs
52
53 exhibited negative cooperativities of ternary complex formation, meaning that they bound the
54
55
56
57
58
59
60

1
2
3 first protein more tightly on their own than in the presence of the second protein ($\alpha < 1$,
4
5 where α values are defined as ratio between binary and ternary K_d s,⁵ **Table 1**, see **Figure 3**
6
7 for representative binary and ternary titrations of VCB into **10** in the absence and presence of
8
9 bromodomain).
10



11
12
13
14
15
16
17
18
19
20
21
22
23
24
25
26
27
28
29
30
31
32 **Figure 3. Measuring cooperativities of ternary complex formation by ITC.** (a) VCB
33 titrated into **10** alone. (b) VCB titrated into Brd4^{BD2}-**10** binary complex and (c) VCB titrated
34 into Brd2^{BD1}-**10**. VCB binds more strongly to **10** alone ($K_d = 110$ nM) than to Brd4^{BD2}-**10** (K_d
35 = 180 nM) or Brd2^{BD1}-**10** ($K_d = 330$ nM), highlighting negative cooperativity.
36

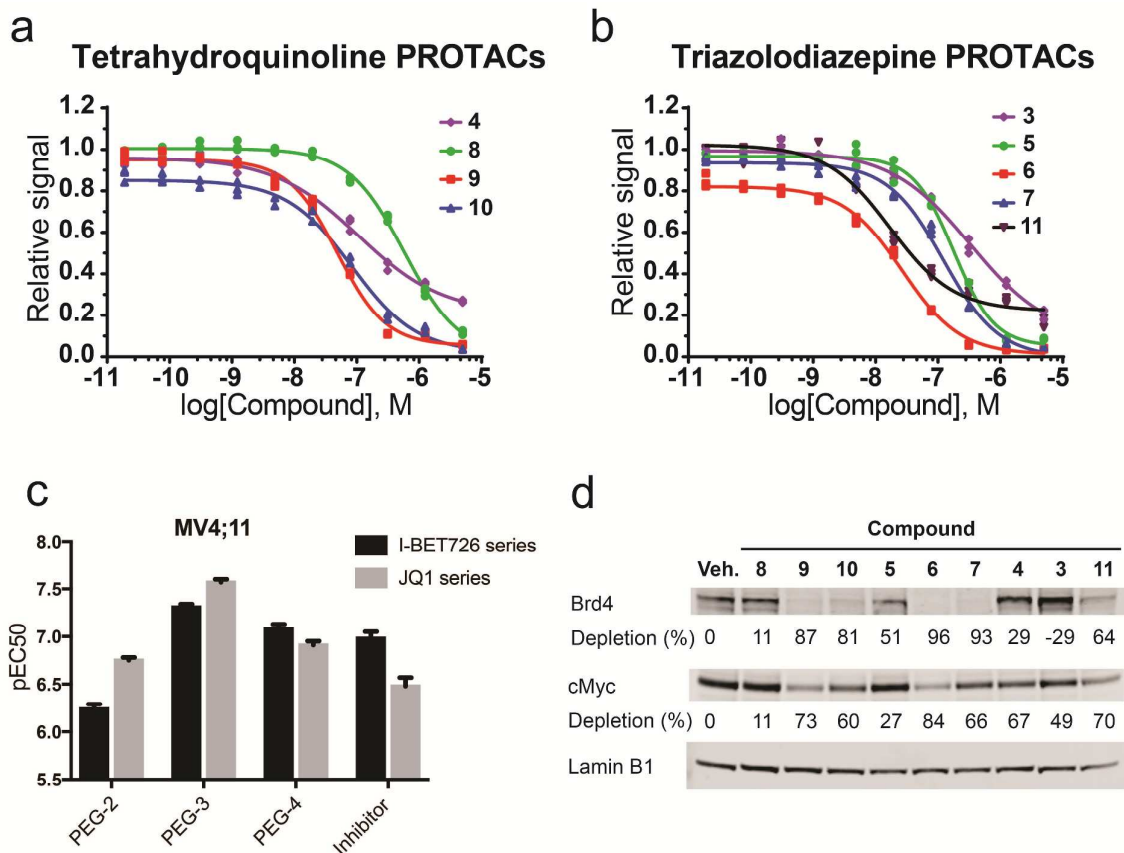
37
38 Negative cooperativities were confirmed against all six BET bromodomains, as shown for
39 representative compound **10**, with the Brd2 bromodomains showing the lowest α values
40
41 (**Table S1**). This feature was in stark contrast to the triazolodiazepine-based series **5–7**,
42
43 which all showed positive cooperativities (α values > 1 , **Table 1**). The thermodynamic data
44
45 highlight an important feature; that is, cooperativities of PROTACs ternary complex
46
47 formation do not follow the binding affinities of the target warheads. Our data exemplifies
48
49 how PROTACs made from more potent target warhead ligands can form ternary complexes
50
51 less productively. It is interesting that despite being negatively cooperative, compounds **8–10**
52
53 can still act as effective degraders at low concentration, underscoring the power of the sub-
54
55
56
57
58
59
60

1
2
3 stoichiometric catalytic activity of PROTACs. The observation of stronger hook effects for
4
5 **8–10** compared to **5–7** in the degradation assays is however consistent with their negative
6
7 cooperativity, i.e. with them behaving more like inhibitors than degraders at higher
8
9 concentration. We previously demonstrated the importance of the ligand-induced protein-
10
11 protein contacts in dictating the large positive cooperativity of the VHL:**6**:Brd4 system.⁵ It is
12
13 therefore likely that the different exit vector from the tetrahydroquinoline warhead forces an
14
15 unfavourable relative orientation between the E3 ligase and the bromodomain. Comparing
16
17 the different linker lengths within a given series, it was found that PEG-3 linked **6** showed the
18
19 highest cooperativity amongst the triazolodiazepine-based series, whereas PEG-2 linked **8**
20
21 showed the lowest cooperativity amongst the tetrahydroquinoline-based series (**Table 1**). In
22
23 both series overall, short linker proved to be less efficient in forming ternary complex and
24
25 inducing protein degradation.
26
27
28

29
30 To provide a functional downstream readout of the cellular activity of BET degraders,
31
32 we assessed anti-proliferative effects of PROTACs in AML MV4;11 (**Figure 4a-b**) and
33
34 HL60 (**Fig. S4a-b**), as these are well characterized BET-sensitive cell lines (see full blots in
35
36 **Fig. S6**). All compounds showed marked anti-proliferative activity in both cell lines.
37
38 Although some PROTAC compounds exhibited comparable nanomolar half-maximal anti-
39
40 proliferative concentrations (pEC50s) relative to the constitutive inhibitors alone, the
41
42 maximal response to baseline level at the higher concentrations (E_{max}) of all VHL-based
43
44 PROTACs presented exceeded that of the BET inhibitors (see **Figure 4a-b** and **Fig. S4a-b**,
45
46 and values tabulated in **Table 2**). This activity is likely owing to the more profound effect
47
48 associated with removing the entire protein compared to blocking an individual binding site,
49
50 which leaves other parts and domains of the proteins (e.g. the extra-terminal ET domain) still
51
52 functional. PEG-3 and PEG-4 based PROTACs proved overall more potent than PEG-2,
53
54
55
56
57
58
59
60

consistent with the trends in degradation activities in HeLa and cooperativities (**Figure 4c** and **Table 2**).

To confirm Brd4 degradation and downstream impact on cMyc levels, we examined protein levels in the same cellular context following acute pharmacological intervention (4 h treatments). In each of the two series, PEG-3 and PEG-4 based PROTACs (**6** and **7**, **9** and **10**) induced superior depletion of both Brd4 and cMyc over their respective PEG-2 analogues **5** and **8** in both cell lines, at two different concentrations (**Figure 4d** and **Fig. S4c-e**). PROTACs **6** and **7** and **9** also showed higher depletion of cMyc levels compared to their inhibitor counterparts, indicating a greater downstream response with more efficient chemical degraders, while **5** and **8** induce lower cMyc depletion than the corresponding inhibitors **3** and **4**, respectively (**Fig. 4c**). Together, the results confirmed the PEG-2 linker length to be too short for optimal PROTAC activity.



1
2
3 **Figure 4. Anti-proliferative and Myc-suppression activity of BET degraders and**
4 **inhibitors.** (a-b) MV4;11 cells were treated with PROTACs and their corresponding BET
5 targeting ligands for 48 h prior to quantitation of cell viability. (c) Half-effective
6 concentrations of BET degraders and corresponding inhibitors; (d) MV4;11 cells were treated
7 for 4 h with BET PROTACs or inhibitors (50 nM) or DMSO control. Protein levels are
8 shown from one representative of two biological replicates.
9

10
11
12 Structure-activity relationships (SARs) are typically quantified by measuring binding
13 or inhibition constants (K_d , K_i), or inhibitory dose response curves (IC_{50}). Because induced
14 protein degradation features catalytic depletion of protein levels over time, different
15 parameters are needed to quantify compounds potency and efficacy. To evaluate SAR in a
16 quantitative fashion, we evaluated: pDC_{50} (concentration causing 50% reduction of protein
17 level relative to vehicle) and D_{max} (maximum reduction of protein level relative to vehicle)
18 for HeLa protein degradation responses; pEC_{50} (half-maximal effective concentrations) and
19 E_{max} (maximal response to baseline level at the highest concentrations) from cell viability
20 assays; % reduction of Brd4 and cMyc levels in AML cell lines; and cooperativity (α) of
21 ternary complex formation with VCB and Brd4^{BD2} (values reported in **Table 2**). To evaluate
22 the main drivers of the observed anti-proliferative effects, we plotted PROTACs pEC_{50}
23 values from AML cell viability assays relative to other parameters (**Figure 4**). Strong
24 correlation was found between pEC_{50} in MV4;11 and pDC_{50} on the long isoform of Brd4 in
25 HeLa ($r^2 = 0.84$, **Figure 4a**). The anti-proliferative activities against AML of BET PROTACs
26 and their parent inhibitors correlated well with depletion of cellular levels of cMyc in both
27 MV4;11 ($r^2 = 0.69$, **Figure 4b**) and HL60 ($r^2 = 0.62$), consistent with AML cells proliferation
28 being cMyc-driven.³⁸ Overall, PEG-3 linked **6** and **9** confirmed to be the most effective
29 amongst the VHL-based PROTACs, with activities comparable to those of CRBN-based
30 PROTAC **11**. Importantly, for a given linker length, the trends confirmed
31 tetrahydroquinoline-based PROTACs to be less effective degraders than the triazolodiazepine
32
33
34
35
36
37
38
39
40
41
42
43
44
45
46
47
48
49
50
51
52
53
54
55
56
57
58
59
60

based, despite the constitutive ligand **4** confirming to be a more potent BET inhibitor than **3** in these cell lines (Figure 4c).

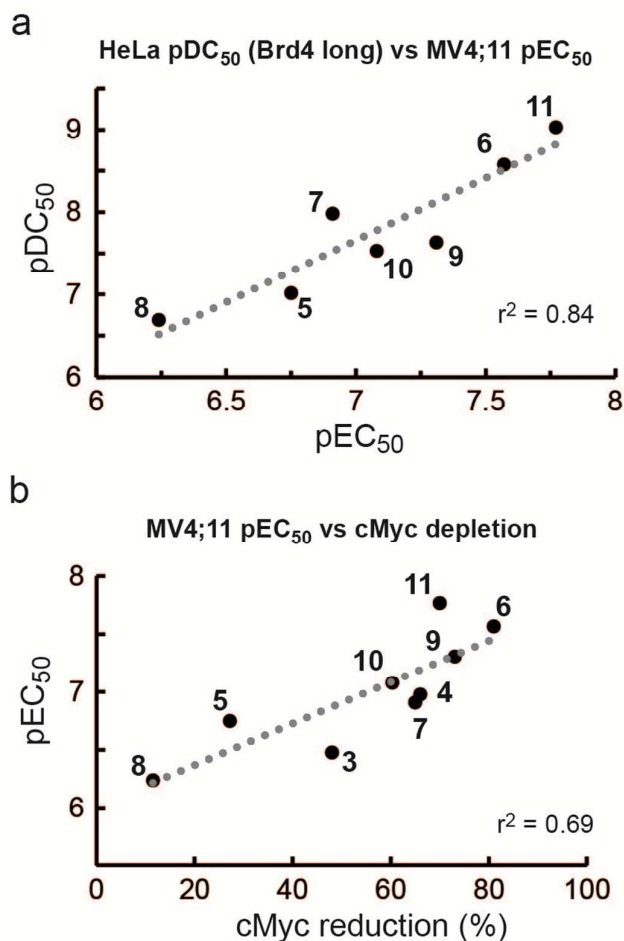


Figure 5. PROTACs' SAR correlation plots. Anti-AML activities (48 h treatments) plotted against (a) HeLa degradation of Brd4 long isoform (24 h), and (b) reduction in cMyc levels in MV4;11 (4 h).

CONCLUSIONS

We describe novel VHL-targeting BET degraders designed based on a high-affinity tetrahydroquinoline inhibitor, and explore the impact of varying the BET-recruiting scaffold and the linkage vector on PROTAC ternary complex recognition and cellular activity. Despite being derivatized from a more potent BET inhibitor, the tetrahydroquinoline based series showed negative cooperativities of ternary complex formation and proved to be less effective degraders than the positively cooperative triazolodiazepine series. These results

1
2
3 exemplify how more potent inhibitors do not necessarily generate more potent PROTACs,
4
5 and underscore how the ability to strongly form the ternary complex is critical to the
6
7 mechanism of action of bivalent degraders. Side-by-side comparisons demonstrated
8
9 remarkable dependency of cellular activity on the linker length, with a trend of PEG-3 >
10
11 PEG-4 >> PEG-2 observed for both chemical series, potentially suggesting a “sweet-spot”
12
13 for optimal linking within a given E3 ligase:target pair. We also show how by changing the
14
15 BET-recruiting warhead and linkage vector, the intra-BET degradation selectivity profile
16
17 could be tuned from Brd4-selective for one series to Brd3/4 selective for another. Further
18
19 SAR on either the linker or warhead ligand and exit vector could further increase potency and
20
21 selectivity of degrading the different BET proteins. Future work assessing the impact of
22
23 varying other parameters, such as the nature of the E3 ligase recruited and the E3 warhead
24
25 used is also warranted. More generally, we provide a framework for establishing future
26
27 structure-activity relationships of chemical degraders based on measurable in vitro
28
29 parameters that we anticipate will prove useful to the burgeoning new field of inducing
30
31 protein degradation with small molecules.
32
33
34
35
36
37

38 EXPERIMENTAL SECTION

39 A. Chemistry

40
41 All chemicals, unless otherwise stated were commercially available and used without
42
43 further purification. Enantiopure (+)-**3** and **4** were purchased from Medchemexpress LLC,
44
45 Princeton, USA. (+)-**3** was deprotected to the carboxylic acid form 6H-Thieno[3,2-
46
47 f][1,2,4]triazolo[4,3-a][1,4]diazepine-6-acetic acid, as previously described.¹⁶ **11** was
48
49 synthesized as described previously.²² **6** and **7** were synthesized as described.¹⁶ Reactions
50
51 were magnetically stirred; commercially available anhydrous solvents were used. NMR
52
53 spectra were recorded on a Bruker Ascend 400. Chemical shifts are quoted in ppm and
54
55
56
57
58
59
60

1
2
3 referenced to the residual solvent signals: ^1H δ = 7.26 (CDCl_3), ^{13}C δ = 77.16; signal splitting
4
5 patterns are described as singlet (s), doublet (d), triplet (t), quartet (q), multiplet (m), broad
6
7 (br). Coupling constants ($J_{\text{H-H}}$) are measured in Hz. High Resolution Mass Spectra (HRMS)
8
9 were recorded on a Bruker microTOF. Low resolution MS and analytical HPLC traces were
10
11 recorded on an Agilent Technologies 1200 series HPLC connected to an Agilent
12
13 Technologies 6130 quadrupole LC-MS, connected to an Agilent diode array detector.
14
15 Preparative HPLC was performed on a Gilson Preparative HPLC System with a Waters X-
16
17 Bridge C18 column (100 mm x 19 mm; 5 μm particle size) and a gradient of 5 % to 95 %
18
19 acetonitrile in water over 10 min, flow 25 mL/min, with 0.1 % ammonia in the aqueous
20
21 phase. The purity of all compounds was analyzed by HPLC-MS (ESI) and was > 95%.
22
23

24
25 **General procedure for synthesis of VHL ligand–linker conjugates.** The azide-(PEG) n
26
27 derivatives of compound **1** were synthesized as previously described.¹⁶
28

29
30 **(2*S*,4*R*)-1-((*S*)-2-(2-(2-(2-Azidoethoxy)ethoxy)acetamido)-3,3-dimethylbutanoyl)-4-**
31
32 **hydroxy-*N*-(4-(4-methylthiazol-5-yl)benzyl)pyrrolidine-2-carboxamide.** Prepared
33
34 accordingly to the general procedure for synthesis of VHL ligand–linker conjugates.
35
36 Obtained 411 mg, colorless oil, 68% yield. $^1\text{H-NMR}$ (CDCl_3 , 400 MHz) δ ppm: 8.68 (s,
37
38 1H), 7.38–7.33 (m, 5H), 7.24 (d, J = 8.5 Hz, 1H), 4.75 (t, J = 7.9 Hz, 1H), 4.59–4.54 (m,
39
40 2H), 4.48 (d, J = 8.6 Hz, 1H), 4.33 (dd, J = 14.9 Hz, J = 5.2 Hz, 1H), 4.12–4.09 (m, 1H),
41
42 4.06–3.96 (m, 2H), 3.70–3.66 (m, 6H), 3.61 (dd, J = 11.4 Hz, J = 3.7 Hz, 1H), 3.41–3.38 (m,
43
44 2H), 2.89 (br s, 1H), 2.63–2.58 (m, 1H), 2.52 (s, 3H), 2.13–2.08 (m, 1H), 0.95 (s, 9H); $^{13}\text{C-}$
45
46 NMR (CDCl_3 , 101 MHz) δ ppm: 171.6, 170.7, 170.6, 150.7, 138.4, 130.4, 129.7, 128.6,
47
48 128.4, 127.6, 71.2, 70.5, 70.3, 70.2, 67.2, 58.5, 57.3, 56.8, 50.7, 43.4, 35.8, 34.9, 26.5, 16.0.
49
50 MS calc. for $\text{C}_{28}\text{H}_{39}\text{N}_7\text{O}_6\text{S}$ 601.3, found 602.3 [$\text{M}+\text{H}^+$].
51
52

53
54 **General procedure for synthesis of final PROTAC molecules.** The azide-(PEG) n
55
56 derivative of compound **1** (40 μmol) was dissolved in methanol (5 ml). Catalytic amount of
57
58
59
60

1
2
3 Pd on charcoal (10 %, dry) was added and the reaction mixture stirred under an atmosphere
4 of hydrogen for 3 h at 25 °C. The reaction mixture was filtered through a plug of celite and
5 the resulting solution evaporated to dryness to obtain the desired amine. The resulting
6 amines (35 μ mol, 1.4 eq.) and **4** or the carboxylic acid form of (+)-**3** (25 μ mol, 1 eq.) were
7 dissolved in DCM (2 ml). HATU (14.3 mg, 37.5 μ mol, 1.5 eq.) was added and the pH
8 adjusted to >9 by adding DIPEA (17.5 μ l, 100 μ mol, 4 eq.). After stirring the reaction
9 mixture at 25 °C for 18 h the solvent was removed in vacuum. The crude was purified by
10 preparative HPLC as described above.
11
12
13
14
15
16
17
18
19
20

21
22 **(2*S*,4*R*)-1-((*S*)-2-(*Tert*-butyl)-14-((*S*)-4-(4-chlorophenyl)-2,3,9-trimethyl-6*H*-**
23 **thieno[3,2-*f*][1,2,4]triazolo[4,3-*a*][1,4]diazepin-6-yl)-4,13-dioxo-6,9-dioxa-3,12-**
24 **diazatetradecanoyl)-4-hydroxy-*N*-(4-(4-methylthiazol-5-yl)benzyl)pyrrolidine-2-**
25 **carboxamide (5).** White amorphous powder. Yield: 22.2 mg (66 %); ¹H-NMR (CDCl₃, 400
26 MHz) δ ppm: 8.65 (s, 1H), 8.30–8.25 (m, 2H), 7.63 (d, *J* = 10.0 Hz, 1H), 7.36 (d, *J* = 8.7 Hz,
27 2H), 7.24 (d, *J* = 8.3 Hz, 2H), 7.11 (d, *J* = 8.0 Hz, 2H), 7.02 (d, *J* = 8.0 Hz, 2H), 4.94–4.86
28 (m, 2H), 4.63–4.57 (m, 2H), 4.21 (d, *J* = 5.8 Hz, 2H), 4.07–3.81 (m, 5H), 3.72–3.52 (m, 7H),
29 3.44 (dd, *J* = 15.9 Hz, *J* = 3.0 Hz, 1H), 3.13–3.08 (m, 1H), 2.55 (s, 3H), 2.45 (s, 3H), 2.39–
30 2.35 (m, 4H), 2.27–2.20 (m, 1H), 1.66 (s, 3H), 1.09 (s, 9 H); ¹³C-NMR (CDCl₃, 101 MHz) δ
31 ppm: 172.1, 171.1, 170.6, 170.4, 163.3, 156.2, 150.2, 149.9, 148.4, 138.5, 136.9, 136.7,
32 131.9, 131.6, 131.4, 131.3, 131.2, 130.2, 130.1, 129, 128.8, 127.7, 71.5, 70.4, 70.3, 69.8,
33 59.3, 57.5, 56.5, 53.9, 42.7, 39.7, 38.3, 37.2, 36.3, 26.6, 16.2, 14.5, 13.3, 11.8. HRMS *m/z*
34 calc. for C₄₆H₅₇N₉ClO₇S₂ expected 957.3505, found 958.3498 [M+H⁺].
35
36
37
38
39
40
41
42
43
44
45
46
47
48
49

50
51 ***S*,4*R*)-1-((*S*)-1-(4-((2*S*,4*R*)-1-Acetyl-4-((4-chlorophenyl)amino)-2-methyl-1,2,3,4-**
52 **tetrahydroquinolin-6-yl)phenyl)-12-(*tert*-butyl)-1,10-dioxo-5,8-dioxa-2,11-**
53 **diazatridecan-13-oyl)-4-hydroxy-*N*-(4-(4-methylthiazol-5-yl)benzyl)pyrrolidine-2-**
54 **carboxamide (8).** White amorphous powder. Yield: 14.5 mg (42 %). ¹H-NMR (CDCl₃, 400
55 MHz) δ ppm: 8.65 (s, 1H), 8.30–8.25 (m, 2H), 7.63 (d, *J* = 10.0 Hz, 1H), 7.36 (d, *J* = 8.7 Hz,
56 2H), 7.24 (d, *J* = 8.3 Hz, 2H), 7.11 (d, *J* = 8.0 Hz, 2H), 7.02 (d, *J* = 8.0 Hz, 2H), 4.94–4.86
57 (m, 2H), 4.63–4.57 (m, 2H), 4.21 (d, *J* = 5.8 Hz, 2H), 4.07–3.81 (m, 5H), 3.72–3.52 (m, 7H),
58 3.44 (dd, *J* = 15.9 Hz, *J* = 3.0 Hz, 1H), 3.13–3.08 (m, 1H), 2.55 (s, 3H), 2.45 (s, 3H), 2.39–
59 2.35 (m, 4H), 2.27–2.20 (m, 1H), 1.66 (s, 3H), 1.09 (s, 9 H); ¹³C-NMR (CDCl₃, 101 MHz) δ
60 ppm: 172.1, 171.1, 170.6, 170.4, 163.3, 156.2, 150.2, 149.9, 148.4, 138.5, 136.9, 136.7,
131.9, 131.6, 131.4, 131.3, 131.2, 130.2, 130.1, 129, 128.8, 127.7, 71.5, 70.4, 70.3, 69.8,
59.3, 57.5, 56.5, 53.9, 42.7, 39.7, 38.3, 37.2, 36.3, 26.6, 16.2, 14.5, 13.3, 11.8. HRMS *m/z*

1
2
3 MHz) δ ppm: 8.66 (s, 1H), 7.91 (d, $J = 8.2$ Hz, 2H), 7.79–7.77 (m, 1H), 7.60–7.50 (m, 5H),
4
5 7.32 (d, $J = 7.9$ Hz, 2H), 7.22 (d, $J = 8.1$ Hz, 2H), 7.13 (d, $J = 9.0$ Hz, 2H), 6.63–6.57 (m,
6
7 3H), 4.89 (br. s, 1H), 4.54–4.37 (m, 4H), 4.22–4.15 (m, 2H), 4.07–3.90 (m, 3H), 3.81–3.47
8
9 (m, 10H), 3.20 (br. s, 1H), 2.71–2.64 (m, 1H), 2.50 (s, 3H), 2.38–2.32 (m, 1H), 2.24 (s, 3H),
10
11 1.99–1.93 (m, 1H), 1.36–1.25 (m, 1H), 1.18 (d, $J = 6.4$ Hz, 3H), 0.85 (s, 9H); ^{13}C -NMR
12
13 (CDCl_3 , 101 MHz) δ ppm: 171.1, 170.7, 170.6, 169.4, 167.5, 150.3, 148.5, 145.8, 143.4,
14
15 137.8, 136.3, 133.4, 131.5, 131.0, 129.5, 129.4, 128.3, 128.1, 126.9, 126.6, 126.0, 122.9,
16
17 122.4, 114.5, 77.3, 77.0, 76.7, 71.7, 70.9, 70.7, 70.5, 70.0, 58.8, 57.0, 56.9, 50.5, 43.3, 41.1,
18
19 39.8, 36.2, 36.0, 26.4, 23.1, 21.3, 16.1; HRMS m/z calc. for $\text{C}_{53}\text{H}_{63}\text{ClN}_7\text{O}_8\text{S}$ [$\text{M}+\text{H}^+$]
20
21 992.4142, found 992.4091.
22
23

24
25 ***S,4R***-1-((*S*)-1-(4-((*2S,4R*)-1-Acetyl-4-((4-chlorophenyl)amino)-2-methyl-1,2,3,4-
26
27 tetrahydroquinolin-6-yl)phenyl)-15-(*tert*-butyl)-1,13-dioxo-5,8,11-trioxa-2,14-
28
29 diazahexadecan-16-oyl)-4-hydroxy-*N*-(4-(4-methylthiazol-5-yl)benzyl)pyrrolidine-2-
30
31 carboxamide (**9**). White amorphous powder. Yield: 17.1 mg (71 %). ^1H -NMR (CDCl_3 , 400
32
33 MHz) δ ppm: 8.66 (s, 1H), 7.80 (d, $J = 8.5$ Hz, 2H), 7.53–7.48 (m, 4H), 7.36–7.30 (m, 6H),
34
35 7.22–7.19 (m, 2H), 7.14 (d, $J = 8.7$ Hz, 2H), 6.64 (d, $J = 8.6$ Hz, 2H), 4.88 (br. s, 1H), 4.60
36
37 (t, $J = 7.7$ Hz, 1H), 4.52 (d, $J = 19.7$ Hz, 2H), 4.42 (br. s, 1H), 4.34–4.18 (m, 3H), 3.94–3.72
38
39 (m, 3H), 3.68–3.51 (m, 14H), 3.21 (br. s, 1H), 2.70–2.64 (m, 1H), 2.49 (s, 3H), 2.44–2.36
40
41 (m, 1H), 2.22 (s, 3H), 2.05–2.01 (m, 1H), 1.34–1.25 (m, 1H), 1.18 (d, $J = 6.3$ Hz, 3H), 0.94
42
43 (s, 9H); ^{13}C -NMR (CDCl_3 , 101 MHz) δ ppm: 171.1, 170.9, 170.2, 169.5, 167.4, 150.3,
44
45 145.8, 143.2, 138.2, 137.7, 136.3, 133.4, 130.9, 129.5, 129.3, 128.1, 127.8, 126.9, 126.5,
46
47 125.8, 122.7, 122.6, 114.6, 77.4, 77.0, 76.7, 71.0, 70.4, 70.3, 70.1, 70.0, 69.6, 58.5, 56.9,
48
49 56.8, 50.2, 47.6, 43.2, 41.0, 40.0, 36.2, 35.4, 26.4, 23.1, 21.3, 16.1; HRMS m/z calc. for
50
51 $\text{C}_{55}\text{H}_{67}\text{ClN}_7\text{O}_9\text{S}$ [$\text{M}+\text{H}^+$] 1036.4404, found 1036.4356.
52
53
54
55
56
57
58
59
60

(2*S*,4*R*)-1-((*S*)-1-(4-((2*S*,4*R*)-1-Acetyl-4-((4-chlorophenyl)amino)-2-methyl-1,2,3,4-tetrahydroquinolin-6-yl)phenyl)-18-(*tert*-butyl)-1,16-dioxo-5,8,11,14-tetraoxa-2,17-diazanonadecan-19-oyl)-4-hydroxy-*N*-(4-(4-methylthiazol-5-yl)benzyl)pyrrolidine-2-carboxamide (10). White amorphous powder. Yield: 14.6 mg (58 %). ¹H-NMR (CDCl₃, 400 MHz) δ ppm: 8.66 (s, 1H), 7.84 (d, *J* = 8.1 Hz, 2H), 7.54–7.49 (m, 4H), 7.36–7.30 (m, 5H), 7.26–7.22 (m, 2H), 7.15–7.12 (m, 3H), 6.62 (d, *J* = 8.6 Hz, 2H), 4.89 (br. s, 1H), 4.69 (t, *J* = 7.9 Hz, 1H), 4.57–4.46 (m, 3H), 4.33 (dd, *J* = 5.6, 14.7 Hz, 1H), 4.24–4.15 (m, 2H), 4.00–3.80 (m, 3H), 3.66–3.55 (m, 18H), 3.46 (br. s, 1H), 2.69–2.63 (m, 1H), 2.50–2.44 (m, 4H), 2.22 (s, 3H), 2.10–2.06 (m, 1H), 1.36–1.25 (m, 1H), 1.18 (d, *J* = 6.2 Hz, 3H), 0.93 (s, 9H); ¹³C-NMR (CDCl₃, 101 MHz) δ ppm: 170.2, 169.5, 167.3, 150.3, 145.8, 143.2, 138.2, 137.8, 136.3, 133.4, 129.5, 129.3, 128.1, 127.8, 126.9, 126.5, 125.9, 122.6, 114.5, 71.0, 70.6, 70.2, 69.8, 58.6, 57.0, 56.8, 50.3, 47.5, 43.2, 41.1, 39.9, 36.1, 35.3, 26.4, 23.1, 21.3, 16.1; HRMS *m/z* calc. for C₅₇H₇₁ClN₇O₁₀S [M+H⁺] 1080.4666, found 1080.4623.

B. BIOLOGY

HeLa cells were kept in DMEM medium (Gibco) supplemented with 10% fetal bovine serum (FBS) (Gibco), L-glutamine (Gibco), penicillin, streptomycin. MV4;11 and HL60 cells were kept in RPMI medium (Gibco) supplemented with 10% FBS, L-glutamine, penicillin and streptomycin. Cells were kept at 37 °C, 5% CO₂.

Testing compounds in cells. HeLa cells were seeded at 3×10^5 per well on a standard 6-well plate. After a day, cells were treated with compounds for the desired time. Cells were washed with PBS twice and lysed with RIPA buffer (Sigma), supplemented with protease inhibitor cocktail (Roche), Benzonase (Merck) and 0.5 mM MgCl₂. Lysate was briefly sonicated and centrifuged at $20000 \times g$ for 10 min at 4 °C. Supernatant was collected and protein concentration measured by BCA assay. For MV4;11 and HL60, 1.2×10^7 cells in 15

1
2
3 mL medium were treated with compound for the desired time. Cells were washed with PBS
4
5 twice, and lysed with hypotonic buffer (10 mM HEPES, 10 mM KCl, protease inhibitor
6
7 cocktail, Benzonase and 0.5 mM MgCl₂) for 30 min by vortexing twice in between the
8
9 incubation period to disrupt cell outer membrane and release nuclei. Nuclei were pelleted by
10
11 centrifugation at 2000 × *g* for 15 min. The pellet was resuspended in RIPA buffer,
12
13 supplemented with protease inhibitor cocktail, Benzonase and 0.5 mM MgCl₂. The
14
15 suspension was briefly sonicated and centrifuged at 20000 × *g* for 10 min at 4 °C.
16
17 Supernatant was collected and protein concentration measured by BCA assay.
18
19

20
21 **Immunoblotting.** Protein on gel was transferred to nitrocellulose membrane using
22
23 iBlot2 (Life technology) according to manufacturer guidelines. Blots were probed with anti-
24
25 Brd4 (AbCam, ab128874), anti-Brd3 (AbCam, ab50818), anti-Brd2 (AbCam, ab139690),
26
27 anti-β-actin (Cell signaling, #4970), anti-cMyc (AbCam, ab32072), anti-lamin B1 (AbCam,
28
29 ab133741) antibodies. Blots were developed with secondary anti-Mouse IgG (Licor, 926-
30
31 32210) or anti-Rabbit IgG (Licor, 926-32213) antibodies from Licor and bands visualized
32
33 using Licor Odessey Sa imaging system.
34
35

36
37 **Western blot quantification.** Image processing and band intensity quantification were
38
39 performed using Licor Image Studio software v5.2.5. Reported band intensities are
40
41 normalized to loading control, i.e. β-actin for total lysates and lamin B1 for nuclear extracts.
42
43 DC₅₀ values were determined by assuming a linear model between the two data points across
44
45 the 50% protein level mark. D_{max} was determined as the highest protein depletion across the
46
47 concentrations tested.
48
49

50
51 **Cell viability assay.** MV4;11 or HL60 cells were incubated with compounds at the
52
53 desired concentration for 48 h on a clear-bottom 384-well plate. Cells were kept in RPMI
54
55 medium supplemented with 10% FBS, L-glutamine, penicillin and streptomycin. Initial cell
56
57 density was 3 × 10⁵ per mL. Cells were treated with various concentration of compound or
58
59
60

1
2
3 0.05% DMSO. After treatment, cell viability was measured with Promega CellTiter-Glo®
4
5 Luminescent Cell Viability Assay kit according to the manufacturer instructions. Signal was
6
7 recorded on a BMG Labtech Pherastar luminescence plate reader with recommended
8
9 settings. Data was analyzed with Graphpad Prism software to obtain EC₅₀ values of each test
10
11 compound.
12

13
14 **Protein expression and purification.** Bromodomain and VCB complex constructs and
15
16 protein preparation were described in previous publication.⁵ Wild-type version of human
17
18 proteins VHL (UniProt accession number: P40337) ElonginC (Q15369), ElonginB (Q15370),
19
20 Brd2 (P25440), Brd3 (Q15059) and Brd4 (O60885) were used for all protein expression. In
21
22 brief, the His₆-tagged constructs were transformed into *E. coli* BL21(DE3) and induced with
23
24 IPTG to produce the desired proteins. *E. coli* cells were homogenized at 4 degree Celsius and
25
26 His₆-tagged proteins were purified from the soluble lysate was by passing through a Ni
27
28 affinity column. After cleaving the His-tag by TEV protease, a second Ni affinity column
29
30 purification was performed to obtain tag-free protein in the flow-through. VCB was then
31
32 additionally purified by anion exchange using MonoQ (GE Healthcare). For all proteins,
33
34 purity was further polished by gel filtration chromatography.
35
36
37

38
39 **Isothermal titration calorimetry (ITC).** Titrations were performed on an ITC200
40
41 micro-calorimeter (GE Healthcare) as previously reported.⁵ The titrations were in ITC buffer
42
43 20 mM Bis-Tris propane, 150 mM NaCl, 1 mM tris(2-carboxyethyl)phosphine (TCEP), pH
44
45 7.4 supplemented with either 0.2% or 3% DMSO and consisted of 19 injections of 2 µl
46
47 protein solution at a rate of 0.5 µl/s at 120 s time intervals. An initial injection of protein (0.4
48
49 µl) was made and discarded during data analysis. All experiments were performed at 25 °C,
50
51 whilst stirring at 600 r.p.m. PROTACs were diluted from a 10 mM DMSO stock solution to
52
53 20 µM in ITC buffer with the final concentration of DMSO to be 0.2% for triazolodiazepine-
54
55 based PROTAC or 3% for tetrahydroquinoline-based PROTAC. Bromodomain protein in the
56
57
58
59
60

1
2
3 same buffer was titrated into the PROTAC in the cell. At the end of the titration, the excess
4
5 of solution was removed from the cell, the syringe was washed and dried, VCB complex (168
6
7 μM , in the same buffer) was loaded in the syringe and titrated into the complex of PROTAC–
8
9 bromodomain. The concentration of the complex in the cell (C) after the first titration (16.8
10
11 μM), was calculated as follows:
12
13

$$C = \frac{C_0 \cdot V_{\text{cell}}}{V_{\text{cell}} + V_{\text{inj}}}$$

14
15
16
17
18
19
20 where: C_0 is the initial concentration of the PROTAC in the cell (20 μM), V_{cell} is the
21
22 volume of the sample cell (200.12 μM) and V_{inj} is the volume of titrant injected during the
23
24 first titration (38.4 μM). Titrations for the binary complex PROTAC–VCB were performed in
25
26 the same manner with VCB titrated into 16.8 μM of PROTAC in the cell. For titration with **8**
27
28 and **9**, concentrations of PROTAC and proteins were halved due to compound solubility. The
29
30 data were fitted to a single-binding-site model to obtain the stoichiometry n , the dissociation
31
32 constant K_d and the enthalpy of binding ΔH using the Microcal LLC ITC200 Origin
33
34 software provided by the manufacturer.
35
36
37
38
39

40 ASSOCIATED CONTENT

41 Supporting Information

42
43 Dose-dependent western blots and quantification of protein levels in HeLa cells; ITC titration
44
45 curves and results; anti-proliferative activities in HL60; Brd4 and cMyc-suppression in
46
47 MV4;11 and HL60; original blot images; NMR spectra of tetrahydroquinoline-based
48
49 PROTACs.
50
51

52
53 Molecular Formula Strings (CSV)
54

55
56 This material is available free of charge on the ACS Publications website.
57
58
59
60

AUTHOR INFORMATION**Corresponding Author**

* Phone: +44 (0)1382 386230. E-mail: a.ciulli@dundee.ac.uk

Author Contributions

All authors have given approval to final version of the manuscript.

Funding Sources

This work was supported by the European Research Council (ERC-2012-StG-311460 DrugE3CRLs Starting Grant to A.C.); the UK Biotechnology and Biological Sciences Research Council (BBSRC grant BB/J001201/2 to A.C.); the European Commission (H2020- MSCA-IF-2014-655516 Marie Skłodowska-Curie Actions Individual Fellowship to K-H.C.); and the Wellcome Trust (Strategic Awards 100476/Z/12/Z for biophysics and drug discovery to the Division of Biological Chemistry and Drug Discovery).

Notes

The authors declare no competing financial interests.

ACKNOWLEDGMENTS

We are thankful to L. Finn for support with tissue culture (MRC-PPU), and the Ferguson lab for access to LI-COR equipment.

ABBREVIATIONS USED

1
2
3 BET, bromodomain and extra-terminal; Brd2/3/4, bromodomain-containing protein 2/3/4;
4
5 CRBN, cereblon; DIPEA *N,N*-diisopropylethylamine; HATU 1-
6
7 [bis(dimethylamino)methylene]-1*H*-1,2,3-triazolo[4,5-*b*]pyridinium 3-oxid
8
9 hexafluorophosphate; PROTAC, proteolysis-targeting chimera; VHL, von Hippel-Lindau
10
11
12
13
14
15

16 REFERENCES

- 17
18 (1) Huang, X.; Dixit, V. M. Drugging the Undruggables: Exploring the Ubiquitin
19 System for Drug Development. *Cell Res.* **2016**, *26* (4), 484–498.
20
21
22 (2) Lai, A. C.; Crews, C. M. Induced Protein Degradation: an Emerging Drug Discovery
23 Paradigm. *Nat. Rev. Drug Discov.* **2017**, *16* (2), 101–114.
24
25
26 (3) Collins, I.; Wang, H.; Caldwell, J. J.; Chopra, R. Chemical Approaches to Targeted
27 Protein Degradation Through Modulation of the Ubiquitin-Proteasome Pathway.
28
29
30
31
32
33
34 (4) Ottis, P.; Crews, C. M. Proteolysis-Targeting Chimeras: Induced Protein Degradation
35 as a Therapeutic Strategy. *ACS Chem. Biol.* **2017**, *12* (4), 892–898.
36
37
38 (5) Gadd, M. S.; Testa, A.; Lucas, X.; Chan, K.-H.; Chen, W.; Lamont, D. J.; Zengerle,
39 M.; Ciulli, A. Structural Basis of PROTAC Cooperative Recognition for Selective
40
41
42
43
44
45
46 (6) Sakamoto, K. M.; Kim, K. B.; Kumagai, A.; Mercurio, F.; Crews, C. M.; Deshaies,
47 R. J. Protacs: Chimeric Molecules That Target Proteins to the Skp1-Cullin-F Box
48
49
50
51
52
53
54
55 (7) Schneekloth, J. S.; Fonseca, F. N.; Koldobskiy, M.; Mandal, A.; Deshaies, R.;
56
57
58
59
60
Sakamoto, K.; Crews, C. M. Chemical Genetic Control of Protein Levels: Selective

- 1
2
3 in Vivo Targeted Degradation. *J. Am. Chem. Soc.* **2004**, *126* (12), 3748–3754.
4
5 (8) Bulatov, E.; Ciulli, A. Targeting Cullin-RING E3 Ubiquitin Ligases for Drug
6
7 Discovery: Structure, Assembly and Small-Molecule Modulation. *Biochem. J.* **2015**,
8
9 *467* (3), 365–386.
10
11 (9) Buckley, D. L.; Van Molle, I.; Gareiss, P. C.; Tae, H. S.; Michel, J.; Noblin, D. J.;
12
13 Jorgensen, W. L.; Ciulli, A.; Crews, C. M. Targeting the Von Hippel-Lindau E3
14
15 Ubiquitin Ligase Using Small Molecules to Disrupt the VHL/HIF-1 α Interaction. *J.*
16
17 *Am. Chem. Soc.* **2012**, *134* (10), 4465–4468.
18
19 (10) Galdeano, C.; Gadd, M. S.; Soares, P.; Scaffidi, S.; Van Molle, I.; Birced, I.; Hewitt,
20
21 S.; Dias, D. M.; Ciulli, A. Structure-Guided Design and Optimization of Small
22
23 Molecules Targeting the Protein-Protein Interaction Between the Von Hippel-Lindau
24
25 (VHL) E3 Ubiquitin Ligase and the Hypoxia Inducible Factor (HIF) Alpha Subunit
26
27 with in Vitro Nanomolar Affinities. *J. Med. Chem.* **2014**, *57* (20), 8657–8663.
28
29 (11) Frost, J.; Galdeano, C.; Soares, P.; Gadd, M. S.; Grzes, K. M.; Ellis, L.; Epemolu, O.;
30
31 Shimamura, S.; Bantscheff, M.; Grandi, P.; Read, K. D.; Cantrell, D. A.; Rocha, S.;
32
33 Ciulli, A. Potent and Selective Chemical Probe of Hypoxic Signalling Downstream
34
35 of HIF-A Hydroxylation via VHL Inhibition. *Nat. Commun.* **2016**, *7*, 13312.
36
37 (12) Fischer, E. S.; Böhm, K.; Lydeard, J. R.; Yang, H.; Stadler, M. B.; Cavadini, S.;
38
39 Nagel, J.; Serluca, F.; Acker, V.; Lingaraju, G. M.; Tichkule, R. B.; Schebesta, M.;
40
41 Forrester, W. C.; Schirle, M.; Hassiepen, U.; Ottl, J.; Hild, M.; Beckwith, R. E. J.;
42
43 Harper, J. W.; Jenkins, J. L.; Thomä, N. H. Structure of the DDB1-CRBN E3
44
45 Ubiquitin Ligase in Complex with Thalidomide. *Nature* **2014**, *512* (7512), 49–53.
46
47 (13) Chamberlain, P. P.; Lopez-Girona, A.; Miller, K.; Carmel, G.; Pagarigan, B.; Chie-
48
49 Leon, B.; Rychak, E.; Corral, L. G.; Ren, Y. J.; Wang, M.; Riley, M.; Delker, S. L.;
50
51 Ito, T.; Ando, H.; Mori, T.; Hirano, Y.; Handa, H.; Hakoshima, T.; Daniel, T. O.;
52
53
54
55
56
57
58
59
60

- 1
2
3 Cathers, B. E. Structure of the Human Cereblon-DDB1-Lenalidomide Complex
4 Reveals Basis for Responsiveness to Thalidomide Analogs. *Nat. Struct. Mol. Biol.*
5
6
7 **2014**, *21* (9), 803–809.
8
- 9
10 (14) Ito, T.; Ando, H.; Suzuki, T.; Ogura, T.; Hotta, K.; Imamura, Y.; Yamaguchi, Y.;
11 Handa, H. Identification of a Primary Target of Thalidomide Teratogenicity. *Science*
12
13 **2010**, *327* (5971), 1345–1350.
14
- 15
16 (15) Lopez-Girona, A.; Mendy, D.; Ito, T.; Miller, K.; Gandhi, A. K.; Kang, J.; Karasawa,
17 S.; Carmel, G.; Jackson, P.; Abbasian, M.; Mahmoudi, A.; Cathers, B.; Rychak, E.;
18 Gaidarova, S.; Chen, R.; Schafer, P. H.; Handa, H.; Daniel, T. O.; Evans, J. F.;
19 Chopra, R. Cereblon Is a Direct Protein Target for Immunomodulatory and
20 Antiproliferative Activities of Lenalidomide and Pomalidomide. *Leukemia* **2012**, *26*
21 (11), 2326–2335.
22
- 23
24 (16) Zengerle, M.; Chan, K.-H.; Ciulli, A. Selective Small Molecule Induced Degradation
25 of the BET Bromodomain Protein BRD4. *ACS Chem. Biol.* **2015**, *10* (8), 1770–1777.
26
- 27
28 (17) Bondeson, D. P.; Mares, A.; Smith, I. E. D.; Ko, E.; Campos, S.; Miah, A. H.;
29 Mulholland, K. E.; Routly, N.; Buckley, D. L.; Gustafson, J. L.; Zinn, N.; Grandi, P.;
30 Shimamura, S.; Bergamini, G.; Faelth-Savitski, M.; Bantscheff, M.; Cox, C.;
31 Gordon, D. A.; Willard, R. R.; Flanagan, J. J.; Casillas, L. N.; Votta, B. J.; Besten,
32 den, W.; Famm, K.; Kruidenier, L.; Carter, P. S.; Harling, J. D.; Churcher, I.; Crews,
33 C. M. Catalytic in Vivo Protein Knockdown by Small-Molecule PROTACs. *Nat.*
34 *Chem. Biol.* **2015**, *11* (8), 611–617.
35
- 36
37 (18) Lai, A. C.; Toure, M.; Hellerschmied, D.; Salami, J.; Jaime-Figueroa, S.; Ko, E.;
38 Hines, J.; Crews, C. M. Modular PROTAC Design for the Degradation of Oncogenic
39 BCR-ABL. *Angew. Chem. Int. Ed. Engl.* **2016**, *55* (2), 807–810.
40
- 41
42 (19) Raina, K.; Lu, J.; Qian, Y.; Altieri, M.; Gordon, D.; Rossi, A. M. K.; Wang, J.; Chen,
43
44
45
46
47
48
49
50
51
52
53
54
55
56
57
58
59
60

- 1
2
3 X.; Dong, H.; Siu, K.; Winkler, J. D.; Crew, A. P.; Crews, C. M.; Coleman, K. G.
4
5 PROTAC-Induced BET Protein Degradation as a Therapy for Castration-Resistant
6
7 Prostate Cancer. *Proc. Natl. Acad. Sci. U. S. A.* **2016**, *113* (26), 7124–7129.
8
9
10 (20) Wurz, R. P.; Dellamaggiore, K.; Dou, H.; Javier, N.; Lo, M.-C.; McCarter, J. D.;
11
12 Mohl, D.; Sastri, C.; Lipford, J. R.; Cee, V. J. A “Click Chemistry Platform” for the
13
14 Rapid Synthesis of Bispecific Molecules for Inducing Protein Degradation. *J. Med.*
15
16 *Chem.* [Online early access]. DOI: 10.1021/acs.jmedchem.6b01781. Published
17
18 Online: Apr 5, 2017. <http://pubs.acs.org/doi/full/10.1021/acs.jmedchem.6b01781>
19
20 (accessed Apr 6, 2017).
21
22
23 (21) Winter, G. E.; Buckley, D. L.; Paulk, J.; Roberts, J. M.; Souza, A.; Dhe-Paganon, S.;
24
25 Bradner, J. E. Phthalimide Conjugation as a Strategy for in Vivo Target Protein
26
27 Degradation. *Science* **2015**, *348* (6241), 1376–1381.
28
29
30 (22) Lu, J.; Qian, Y.; Altieri, M.; Dong, H.; Wang, J.; Raina, K.; Hines, J.; Winkler, J. D.;
31
32 Crew, A. P.; Coleman, K.; Crews, C. M. Hijacking the E3 Ubiquitin Ligase Cereblon
33
34 to Efficiently Target BRD4. *Chem. Biol.* **2015**, *22* (6), 755–763.
35
36
37 (23) Lebraud, H.; Wright, D. J.; Johnson, C. N.; Heightman, T. D. Protein Degradation by
38
39 in-Cell Self-Assembly of Proteolysis Targeting Chimeras. *ACS Cent. Sci.* **2016**, *2*
40
41 (12), 927–934.
42
43 (24) Remillard, D.; Buckley, D. L.; Paulk, J.; Brien, G. L.; Sonnett, M.; Seo, H.-S.;
44
45 Dastierdi, S.; Wühr, M.; Dhe-Paganon, S.; Armstrong, S. A.; Bradner, J. E.
46
47 Degradation of the BAF Complex Factor BRD9 by Heterobifunctional Ligands.
48
49 *Angew. Chem. Int. Ed. Engl.* **2017**, *468*, 1067.
50
51
52 (25) Schiedel, M.; Herp, D.; Hammelmann, S.; Swyter, S.; Lehotzky, A.; Robaa, D.;
53
54 Oláh, J.; Ovádi, J.; Sippl, W.; Jung, M. Chemically Induced Degradation of Sirtuin 2
55
56 (Sirt2) by a Proteolysis Targeting Chimera (PROTAC) Based on Sirtuin Rearranging
57
58
59
60

- 1
2
3 Ligands (SirReals). *J. Med. Chem.* [Online early access]. DOI:
4
5 10.1021/acs.jmedchem.6b01872. Published Online: Apr 5, 2017.
6
7 <http://pubs.acs.org/doi/full/10.1021/acs.jmedchem.6b01872> (accessed Apr 6, 2017).
8
9
10 (26) Zhang, G.; Smith, S. G.; Zhou, M.-M. Discovery of Chemical Inhibitors of Human
11 Bromodomains. *Chem. Rev.* **2015**, *115* (21), 11625–11668.
12
13 (27) Galdeano, C.; Ciulli, A. Selectivity on-Target of Bromodomain Chemical Probes by
14 Structure-Guided Medicinal Chemistry and Chemical Biology. *Future Med. Chem.*
15 **2016**, *8* (13), 1655–1680.
16
17
18 (28) Dawson, M. A.; Prinjha, R. K.; Dittmann, A.; Giotopoulos, G.; Bantscheff, M.;
19 Chan, W.-I.; Robson, S. C.; Chung, C.-W.; Hopf, C.; Savitski, M. M.; Huthmacher,
20 C.; Gudgin, E.; Lugo, D.; Beinke, S.; Chapman, T. D.; Roberts, E. J.; Soden, P. E.;
21 Auger, K. R.; Mirguet, O.; Doehner, K.; Delwel, R.; Burnett, A. K.; Jeffrey, P.;
22 Drewes, G.; Lee, K.; Huntly, B. J. P.; Kouzarides, T. Inhibition of BET Recruitment
23 to Chromatin as an Effective Treatment for MLL-Fusion Leukaemia. *Nature* **2011**,
24 *478* (7370), 529–533.
25
26 (29) Zuber, J.; Shi, J.; Wang, E.; Rappaport, A. R.; Herrmann, H.; Sison, E. A.; Magoon,
27 D.; Qi, J.; Blatt, K.; Wunderlich, M.; Taylor, M. J.; Johns, C.; Chicas, A.; Mulloy, J.
28 C.; Kogan, S. C.; Brown, P.; Valent, P.; Bradner, J. E.; Lowe, S. W.; Vakoc, C. R.
29 RNAi Screen Identifies Brd4 as a Therapeutic Target in Acute Myeloid Leukaemia.
30 *Nature* **2011**, *478* (7370), 524–528.
31
32 (30) Andrieu, G.; Belkina, A. C.; Denis, G. V. Clinical Trials for BET Inhibitors Run
33 Ahead of the Science. *Drug Discovery Today: Technol.* **2016**, *19*, 45–50.
34
35 (31) Vangamudi, B.; Paul, T. A.; Shah, P. K.; Kost-Alimova, M.; Nottebaum, L.; Shi, X.;
36 Zhan, Y.; Leo, E.; Mahadeshwar, H. S.; Protopopov, A.; Futreal, A.; Tieu, T. N.;
37 Peoples, M.; Heffernan, T. P.; Marszalek, J. R.; Toniatti, C.; Petrocchi, A.; Verhelle,
38
39
40
41
42
43
44
45
46
47
48
49
50
51
52
53
54
55
56
57
58
59
60

- 1
2
3 D.; Owen, D. R.; Draetta, G.; Jones, P.; Palmer, W. S.; Sharma, S.; Andersen, J. N.
4
5 The SMARCA2/4 ATPase Domain Surpasses the Bromodomain as a Drug Target in
6
7 SWI/SNF-Mutant Cancers: Insights From cDNA Rescue and PFI-3 Inhibitor Studies.
8
9 *Cancer Res.* **2015**, *75* (18), 3865–3878.
10
11 (32) Shi, J.; Vakoc, C. R. The Mechanisms Behind the Therapeutic Activity of BET
12
13 Bromodomain Inhibition. *Mol. Cell.* **2014**, *54* (5), 728–736.
14
15 (33) Baud, M. G. J.; Lin-Shiao, E.; Cardote, T.; Tallant, C.; Pschibul, A.; Chan, K.-H.;
16
17 Zengerle, M.; Garcia, J. R.; Kwan, T. T. L.; Ferguson, F. M.; Ciulli, A. A Bump-and-
18
19 Hole Approach to Engineer Controlled Selectivity of BET Bromodomain Chemical
20
21 Probes. *Science* **2014**, *346* (6209), 638–641.
22
23 (34) Filippakopoulos, P.; Qi, J.; Picaud, S.; Shen, Y.; Smith, W. B.; Fedorov, O.; Morse,
24
25 E. M.; Keates, T.; Hickman, T. T.; Felletar, I.; Philpott, M.; Munro, S.; McKeown,
26
27 M. R.; Wang, Y.; Christie, A. L.; West, N.; Cameron, M. J.; Schwartz, B.;
28
29 Heightman, T. D.; La Thangue, N.; French, C. A.; Wiest, O.; Kung, A. L.; Knapp, S.;
30
31 Bradner, J. E. Selective Inhibition of BET Bromodomains. *Nature* **2010**, *468* (7327),
32
33 1067–1073.
34
35 (35) Zhou, B.; Hu, J.; Xu, F.; Chen, Z.; Bai, L.; Fernandez-Salas, E.; Lin, M.; Liu, L.;
36
37 Yang, C.-Y.; Zhao, Y.; McEachern, D.; Przybranowski, S.; Wen, B.; Sun, D.; Wang,
38
39 S. Discovery of a Small-Molecule Degradator of Bromodomain and Extra-Terminal
40
41 (BET) Proteins with Picomolar Cellular Potencies and Capable of Achieving Tumor
42
43 Regression. *J. Med. Chem.* [Online early access]. DOI:
44
45 10.1021/acs.jmedchem.6b01816. Published Online: Mar 24, 2017.
46
47 <http://pubs.acs.org/doi/full/10.1021/acs.jmedchem.6b01816> (accessed Mar 25, 2017).
48
49 (36) Gosmini, R.; Nguyen, V. L.; Toum, J.; Simon, C.; Brusq, J.-M. G.; Krysa, G.;
50
51 Mirguet, O.; Riou-Eymard, A. M.; Boursier, E. V.; Trottet, L.; Bamborough, P.;
52
53
54
55
56
57
58
59
60

- 1
2
3 Clark, H.; Chung, C.-W.; Cutler, L.; Demont, E. H.; Kaur, R.; Lewis, A. J.; Schilling,
4
5 M. B.; Soden, P. E.; Taylor, S.; Walker, A. L.; Walker, M. D.; Prinjha, R. K.;
6
7 Nicodeme, E. The Discovery of I-BET726 (GSK1324726A), a Potent
8
9 Tetrahydroquinoline ApoA1 Up-Regulator and Selective BET Bromodomain
10
11 Inhibitor. *J. Med. Chem.* **2014**, *57* (19), 8111–8131.
12
13
14 (37) Wyce, A.; Ganji, G.; Smitheman, K. N.; Chung, C.-W.; Korenchuk, S.; Bai, Y.;
15
16 Barbash, O.; Le, B.; Craggs, P. D.; McCabe, M. T.; Kennedy-Wilson, K. M.;
17
18 Sanchez, L. V.; Gosmini, R. L.; Parr, N.; McHugh, C. F.; Dhanak, D.; Prinjha, R. K.;
19
20 Auger, K. R.; Tummino, P. J. BET Inhibition Silences Expression of MYCN and
21
22 BCL2 and Induces Cytotoxicity in Neuroblastoma Tumor Models. *PLoS ONE* **2013**,
23
24 *8* (8), e72967.
25
26
27 (38) Delgado, M. D.; León, J. Myc Roles in Hematopoiesis and Leukemia. *Genes Cancer*
28
29 **2010**, *1* (6), 605–616.
30
31
32
33
34
35
36
37
38
39
40
41
42
43
44
45
46
47
48
49
50
51
52
53
54
55
56
57
58
59
60

Table 1 – ITC results of binary and ternary complex formation for PROTACs 5 – 10 and Brd4^{BD2} and VCB.

Protein in Syringe	Species in cell	K _d (nM)	ΔG (kcal × mol ⁻¹)	ΔH (kcal × mol ⁻¹)	-TΔS (kcal × mol ⁻¹)	Stoichiometry <i>N</i>	α	ΔpK _d ± uncertainty	No. of replicates
Brd4 ^{BD2}	8*	3 ± 2	-11.7 ± 0.4	-10.0 ± 0.1	-1.71 ± 0.43	0.804 ± 0.003	-	-	1
Brd4 ^{BD2}	9*	4 ± 2	-11.5 ± 0.3	-9.74 ± 0.10	-1.73 ± 0.30	1.15 ± 0.01	-	-	1
Brd4 ^{BD2}	10	8 ± 4	-11.1 ± 0.3	-10.8 ± 0.05	-0.33 ± 0.38	0.86 ± 0.06	-	-	2
Brd4 ^{BD2}	5	17 ± 2	-10.6 ± 0.06	-11.2 ± 0.04	-0.65 ± 0.47	0.81 ± 0.04	-	-	4
Brd4 ^{BD2}	6	26 ± 2	-10.3 ± 0.04	-11.1 ± 0.8	0.77 ± 0.80	0.91 ± 0.06	-	-	3
Brd4 ^{BD2}	7	27 ± 2	-10.3 ± 0.04	-10.6 ± 0.5	0.31 ± 0.53	0.79 ± 0.03	-	-	2
VCB	8*	116 ± 24	-9.46 ± 0.13	-4.07 ± 0.07	-5.39 ± 0.14	1.12 ± 0.01			1
	9*	105 ± 24	-9.52 ± 0.13	-6.18 ± 0.12	-3.34 ± 0.18	0.96 ± 0.01			1
	10	109 ± 8	-9.50 ± 0.04	-8.01 ± 0.25	-1.50 ± 0.21	0.92 ± 0.15			2
VCB	5	147 ± 24	-9.34 ± 0.10	-5.72 ± 0.47	-3.61 ± 0.37	0.8 ± 0.05			3
	6	69 ± 8	-9.77 ± 0.07	-7.76 ± 0.92	-2.02 ± 0.9	0.81 ± 0.07			3
	7	73 ± 15	-9.75 ± 0.13	-8.79 ± 0.42	-0.96 ± 0.29	0.76 ± 0.03			2
VCB	Brd4 ^{BD2} : 8*	781 ± 60	-8.33 ± 0.05	-7.02 ± 0.11	-1.31 ± 0.12	1.07 ± 0.01	0.2	-0.83 ± 0.10	1
	Brd4 ^{BD2} : 9*	228 ± 33	-9.06 ± 0.09	-6.90 ± 0.11	-2.16 ± 0.14	1.44 ± 0.02	0.5	-0.34 ± 0.12	1
	Brd4 ^{BD2} : 10	183 ± 29	-9.20 ± 0.10	-7.58 ± 0.05	-1.62 ± 0.15	0.87 ± 0.02	0.6	-0.22 ± 0.08	2
VCB	Brd4 ^{BD2} : 5	26 ± 7	-10.4 ± 0.2	-5.36 ± 0.77	-5.05 ± 0.62	0.76 ± 0.06	5.7	0.78 ± 0.16	3
	Brd4 ^{BD2} : 6	9 ± 5	-11.1 ± 0.3	-8.47 ± 2.83	-2.59 ± 0.69	0.83 ± 0.04	7.4	0.95 ± 0.29	2
	Brd4 ^{BD2} : 7	15 ± 1	-10.7 ± 0.05	-10.6 ± 1.3	-0.07 ± 1.3	0.76 ± 0.07	4.7	0.66 ± 0.10	2

Values reported are the means ± s.e.m., unless specified otherwise.

* Errors are generated by the Origin program and reflect the quality of the fit between the nonlinear least-squares curve and the experimental data.

Table 2 – BET reduction by PROTACs in HeLa and antiproliferative activity, Brd4/cMyc reduction in AML cells

	pDC50 / Dmax (%) in HeLa cells				pEC50		E _{max} (%)		Brd4 / cMyc depletion (%)		Cooperativity (α)
	Brd4 short	Brd4 long	Brd3	Brd2	MV4;11	HL60	MV4;11	HL60	MV4;11	HL60	Brd4-BD2
8	6.9 / 94	6.7 / 78	6.8 / 74	- / 37	6.24 ±0.05	6.17 ±0.03	88.1 ± 1.0	96.6 ± 0.1	11 / 11	-156 / 14	0.15
9	8.1 / 98	7.6 / 95	7.3 / 91	- / 43	7.31 ±0.03	6.57 ±0.02	94.2 ± 0.2	98.3 ± 0.1	87 / 73	28 / 50	0.46
10	8.1 / 95	7.5 / 93	7.7 / 92	- / 26	7.08 ±0.05	6.37 ±0.03	96.4 ± 0.2	98.3 ± 0.1	81 / 60	22 / 47	0.59
5	7.0 / 96	7.0 / 97	6.5 / 97	6.2 / 93	6.75 ±0.03	5.84 ±0.06	91.4 ± 0.4	91.4 ± 0.3	51 / 27	-172 / 4	5.7
6	8.1 / 98	8.6 / 100	7.0 / 100	7.4 / 98	7.57 ±0.03	6.66 ±0.05	96.1 ± 0.3	92.0 ± 0.4	96 / 84	82 / 68	7.4
7	8.4 / 99	8.0 / 100	6.5 / 99	6.7 / 97	6.91 ±0.04	5.90 ±0.05	95.2 ± 0.1	91.7 ± 0.1	93 / 66	20 / 23	4.7
11	9.2 / 97	9.0 / 100	9.1 / 98	8.2 / 83	7.77 ±0.06	7.46 ±0.03	83.5 ± 2.3	88.0 ± 0.1	64 / 70	32 / 57	n.d.
4	-	-	-	-	6.98 ±0.07	6.69 ±0.06	73.3 ± 0.6	82.4 ± 4.3	29 / 67	-157 / 42	-
3	-	-	-	-	6.48 ±0.09	6.13 ±0.09	79.1 ± 2.5	73.7 ± 2.5	-29 / 49	-243 / 20	-

DC₅₀: concentration in molar causing 50% reduction of protein level relative to vehicle control treatment in 24 h.

D_{max}: maximum reduction of protein level relative to vehicle control treatment

pEC₅₀ was measured after 48 h treatment. Errors on pEC₅₀ values reflect the quality of the curve fitting; Protein depletion % are for 50 nM treatments (4 h) in MV4;11 / HL60 .

n.d. Not determined

Table of Contents Graphic

